To be presented in the *5th Symposium on Building Physics in the Nordic Countries*, Göteborg, 24-26 August 1999

Measurements and simulations of driving rain on the Main Building of the TUE

Fabien J.R. van Mook[1]

1 INTRODUCTION

To design durable building envelopes, knowlegde of the exposure to local outdoor climate is primordial. One of the parameters is driving rain, defined as rain that is carried by wind and driven onto the building envelope. A standard method for building designers to estimate driving rain quantities (BSI 1992) is available only in the UK. There are few other tools and data available, useful for the estimation of driving rain and for laboratory tests of building materials and structures. In the last two decades computational fluid dynamics (c.f.d.) became available. To the author's knowledge, only a single attempt has been made to compare driving rain c.f.d. simulations with wind tunnel experiments (Hangan and Surry 1998).

Since December 1997 full-scale measurements of wind and driving rain on the west facade of the Main Building of the Eindhoven University of Technology (TUE) are carried out, along with reference measurements of wind and rain. The aim is to determine the function of driving rain quantities as function of reference wind and rain parameters. In this paper, results of the full-scale measurements and results of c.f.d. simulations of wind and driving rain of the same situation are presented.

2 DRIVING RAIN

The general model of driving rain used in this study, has been described in van Mook et al. (1997). Such an approach is also used in e.g. Choi (1993), Karagiozis and Hadjisophocleous (1996), Sankaran and Paterson (1995) and Hangan and Surry (1998). A brief summary of quantities and symbols is provided in this section.

The horizontal rain intensity R_h [mm/s] is the rate of rain water falling through a horizontal plane during a certain period in the undisturbed oncoming wind flow, and equals to the

[1]Building Physics group (FAGO), Eindhoven University of Technology (TUE), Postbus 513, 5600 MB Eindhoven, the Netherlands, famo@fago.bwk.tue.nl

summation of the masses of all the drops falling through the plane:

$$R_h = \int_0^\infty \varphi_h(D) dD, \tag{1}$$

with $\varphi_h(D)$ = horizontal drop mass spectrum [kg m^{-2} s^{-1} m^{-1}], i.e. the total mass of raindrops with diameters D [m] falling on a horizontal plane in the undisturbed wind flow.

Before a raindrop impinges on a building facade, it has travelled from the clouds downwards, and its individual trajectory has been determined by the wind field, the gravitational force and drag forces. For drops of size D, a fraction $\eta(D)$ will impinge on a particular position on the facade, and the actual driving rain intensity R_{dr} on the building will thus be:

$$R_{dr} = \int_0^\infty \eta(D)\varphi_h(D) dD, \tag{2}$$

with $\eta(D)$ = catch ratio [-] per drop size.

The driving rain ratio k is defined as:

$$k = \frac{R_{dr}}{R_h}. \tag{3}$$

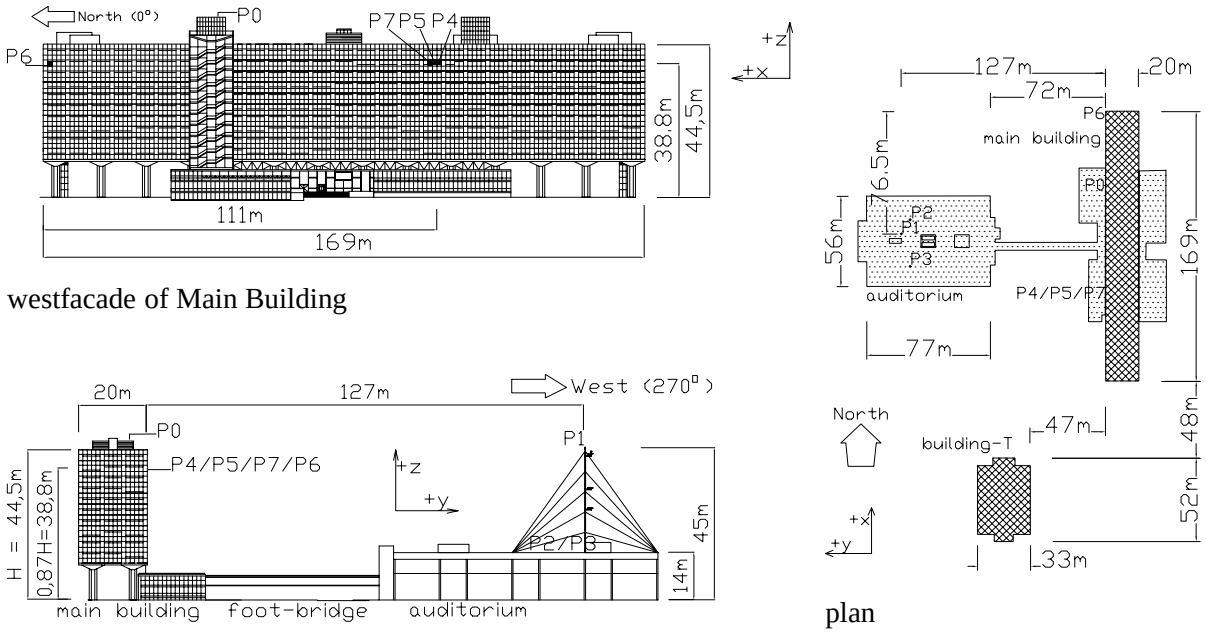

westfacade of Main Building

plan

view from north

Figure 1: Test site, measurement positions P1-P7 and definition of *x*-*y*-*z* axis system.

3 SITE AND MEASUREMENT SET-UP

Full-scale experiments have been carried out at the Main Building on the campus of the TUE. The dimensions of the Main Building are: (height) 44.5 m, (width) 167 m and (depth) 20 m. Figure 1 shows the west facade of the Main Building: driving rain is measured at two positions, P5 and P6, and wind velocity is measured near the facade at position P4.

The site is suited because the prevailing direction for wind and rain is westerly. West from the Main Building there are no large obstacles. The fetch in this section is rough (roughness length of 1 ± 0.4 m, with a displacement height of 10 m (Geurts 1997)), and consists mainly of trees over a distance of 400 m. The nearest high-rise building is building T (45 m high) in south-south-west direction (figure 1). The wind characteristics of the site have been presented in Geurts (1997).

The reference wind velocity is measured at 45 m height (from ground level) on a mast, located 127 m westwards from the Main Building (figure 1, position P1). The mast is standing on the Auditorium, which is 14 m high, 77 m long and 56 m wide, and which is located at 72 m from the Main Building. The reference horizontal rain intensity is measured by two tipping-bucket rain gauges on the roof of the Auditorium at positions P2 and P3. Since December 1998, a disdrometer (a device to measure the raindrop spectrum) has been installed next to one of the tipping-bucket rain gauges (P3). The two driving rain gauges at positions P5 and P6 have been develloped at the TUE. Principle of this type of driving rain gauge and comparison with other types is described in a parallel paper (Högberg et al. 1999). At position P4, an ultrasonic anemometer is mounted at an adjustable distance to the facade surface of 0.25 to 1.25 m.

4 SIMULATION METHOD

4.1 Wind calculation method

Simulations of the wind around the Main Building have been performed by a commercially available c.f.d. package *Fluent* (version 4.4). The used model is a standard K-ε model (Fluent Inc. 1995). Details of the model were described in van Mook (1999). The computational grid is depicted in figure 2. The computational domain is 1190 m long in east-west direction, 1477 m long in north-south direction and 225 m high. It is devided into 95, 96 and 47 cells respectively. The profile of the wind coming into the domain is logarithmic, with roughtness length $z_0 = 1.0$ m and displacement height $d = 10$ m, as determined by measurements on the site (Geurts 1997).

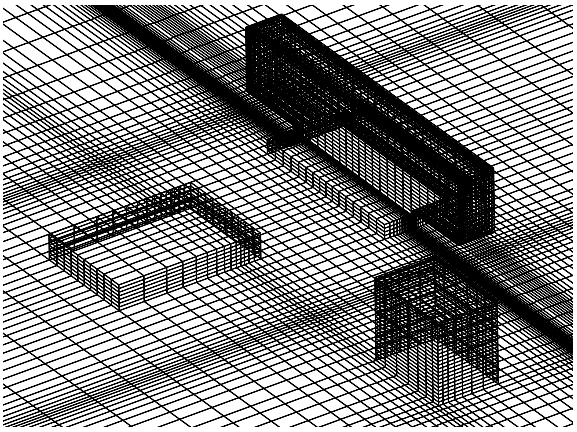

Figure 2: Computational grid. View from south-west. From left to right: the Auditorium, the Main Building and building T.

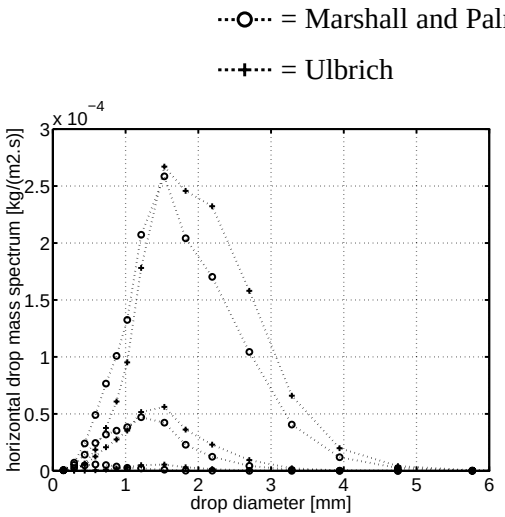

Figure 3: Horizontal drop mass spectrum $\varphi_h(D)$ per drop size interval for reference horizontal rain intensities $R_h = 0.1$, 1.0 and 5.0 mm/h and two raindrop spectra.

4.2 Driving-rain calculation method

The calculations of the drop trajectories were performed after the wind flow calculation, by the same c.f.d. package *Fluent*. A total of ∼20,000 drops (with D = 0.5, 1.0, 1.5, ... 6.0 mm) were released in the computation domain, for every of the three chosen reference wind speeds $U_{h,ref} =$ 3.5, 5.7 and 11.2 m s^{-1} and the two wind directions $\Phi_{ref} = 270^\circ$ (= normal to the facade) and $\Phi_{ref} = 300^\circ$. Horizontal drop mass spectra $\varphi_h(D)$ have been derived from two raindrop spectra known from literature (Marshall and Palmer 1948), (Ulbrich 1983). See figure 3. Dispersion of drops due to the turbulence of wind is not taken into account.

5 RESULTS AND DISCUSSION

5.1 Wind

For conciseness, only one method of comparison between wind measurements en wind simulations is presented here. Other methods were described in van Mook (1999). Figure 4 shows the wind speed at 50 cm from the facade at position P4, $U_{abs,\mathrm{P4}}$, normalised by the horizontal wind speed $U_{h,ref}$ at position P1. The simulated wind speeds $U_{abs,\mathrm{P4}}$ (figure 4) are (just) within the standard deviation of the measurements. The larger deviations are found at wind directions of $< 240^\circ$, due to the wake of building T. Building T (figures 1 and 4.1) has the same height as the Main Building. When building T is included in the computational domain, the results compare better with the measurements. In spite of the imperfections of the standard K-ε model

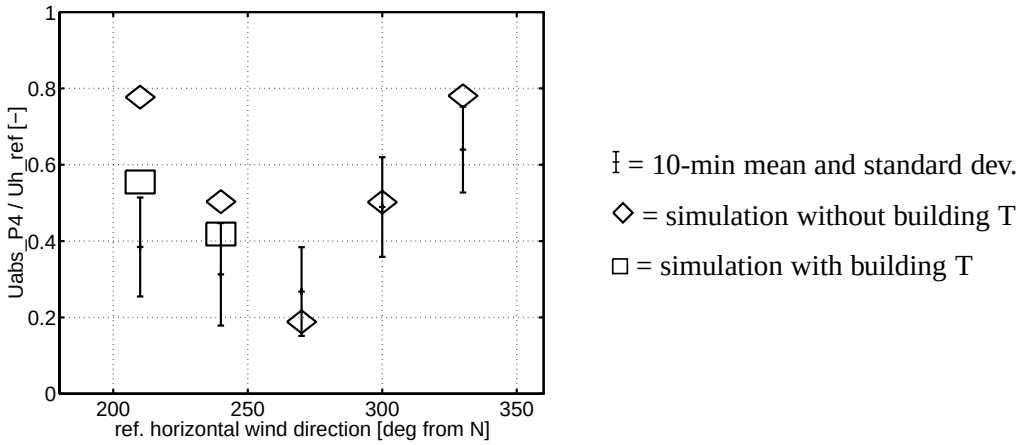

Figure 4: Measured and simulated wind speed $U_{abs,\mathrm{P4}}$ at 50 cm from the facade at position P4, normalised by the reference wind speed $U_{h,ref}$, as function of the reference wind direction Φ_{ref}.

(see e.g. (Murakami et al. 1992)) and the limited number of cells in the computational grid, the simulations of the present study compare within standard deviation of the measurements, so that one can proceed to the driving rain calculations.

5.2 Driving rain

Figure 5a shows measured driving rain ratios k (eq. 3), at facade position P5 as function of the reference wind velocity component normal to the facade ($U_{y,ref}$), measured at P1. The 10-min values in this graph show a large scatter, although the data has been selected by the following criteria: (1) a wind direction $225^\circ \leq \Phi_{ref} \leq 315^\circ$, (2) a maximum r.m.s. wind direction $\sigma_{\Phi_{ref}} < 5^\circ$, (3) a minimum for the reference horizontal rain intensity $R_h \geq 0.02$ mm/h, and, (4) a maximum relative difference in rain intensity R_h, at the two reference positions P2 and P3:

$$\frac{|R_{h,\mathrm{P3}} - R_{h,\mathrm{P2}}|}{R_{h,\mathrm{P2}}} \leq 0.2.$$

By criterium 3 and 4 the relative error in R_h is limited; the other criteria have been defined to make a comparison with the simulation possible.

Figure 5b shows that driving rain ratios do not depend clearly on horizontal rain intensity R_h. This is against the expectation that higher values of R_h yield relatively more larger raindrops and thus higher k. The data in the figure have even been additionally selected for reference wind speeds $5 \leq U_{y,ref} \leq 7$ m s^{-1}. The simulation results (figure 5a), calculated with two different drop spectra, suggest that raindrop spectrum is important: different raindrop spectra with the same rain intensity yield different driving rain ratios.

Several of the simulated catch ratios for $U_{y,ref} < 6$ m s^{-1} are well outside of the standard deviation of the measurements. An explanation might be that the chosen raindrop spectra are not realistic and that dispersion of drops due to turbulence are not taken into account. For a reference wind speed $U_{y,ref} < 4$ m s^{-1}, the overestimation of the simulated driving rain ratio is apparent, and this may to be (also) due to not yet investigated errors in the simulation of wind velocity field and raindrop trajectories.

Measured and simulated driving rain ratios at the edge position P6 are depicted in figure 5c. The measured data were selected in the same way as for position P5. The scatter of the measurements is larger at P6, i.e. 1.9 m from the building edge. Besides, the driving rain ratios at P6 are higher than at P5, as one would expect. Figure 6 shows quotients ($k_{\mathsf{P5}}/k_{\mathsf{P6}}$) of driving rain ratios at P5 and P6 as function of the reference wind direction. The selection criteria were the same as for previous figures. For winds from north to west, more driving rain is falling at the north edge (P6) than at the central position (P5). The inverse applies for winds from west to south. Such a dependency to the wind direction has not been reported in the literature known to the author. The simulations show again a slight overestimation of $k_{\mathsf{P5}}/k_{\mathsf{P6}}$.

6 CONCLUSIONS

Measured 10-min values of driving rain ratio k, i.e. the ratio of driving rain intensity and reference horizontal rain intenisity, show a large scatter, even selected for a refererence wind velocity interval $U_{y,ref}$, a maximum r.m.s. wind direction $\sigma_{\Phi_{ref}}$, and a minimum reference horizontal rain intensity R_h. The standard deviation of k as function of $U_{y,ref}$ is $\sim$50% of the mean value of k. The scatter of 10-min values of k does not only seem to depend on wind velocity and horizontal rain intensity (and their natural variation in space and time) but is presumably also due to variations in raindrop spectra, as is also visible in the simulations. Further research will include raindrop spectrum measurements by a disdrometer to verify this.

A favourable comparison of wind simulations with a K-ε model with wind measurements has been reported more extensively in an other paper (van Mook 1999). Driving rain is simulated with raindrop spectra known from literature. Some of the simulated driving rain ratios are well outside the standard deviation of the measured driving rain ratio, especially at low wind speeds ($U_{y,ref} < 4$ m s^{-1}). A further investigation should bring clarity, whether it is mainly due to errors in the calculation of drop trajectories, due to the chosen raindrop spectra or due to raindrop dispersion.

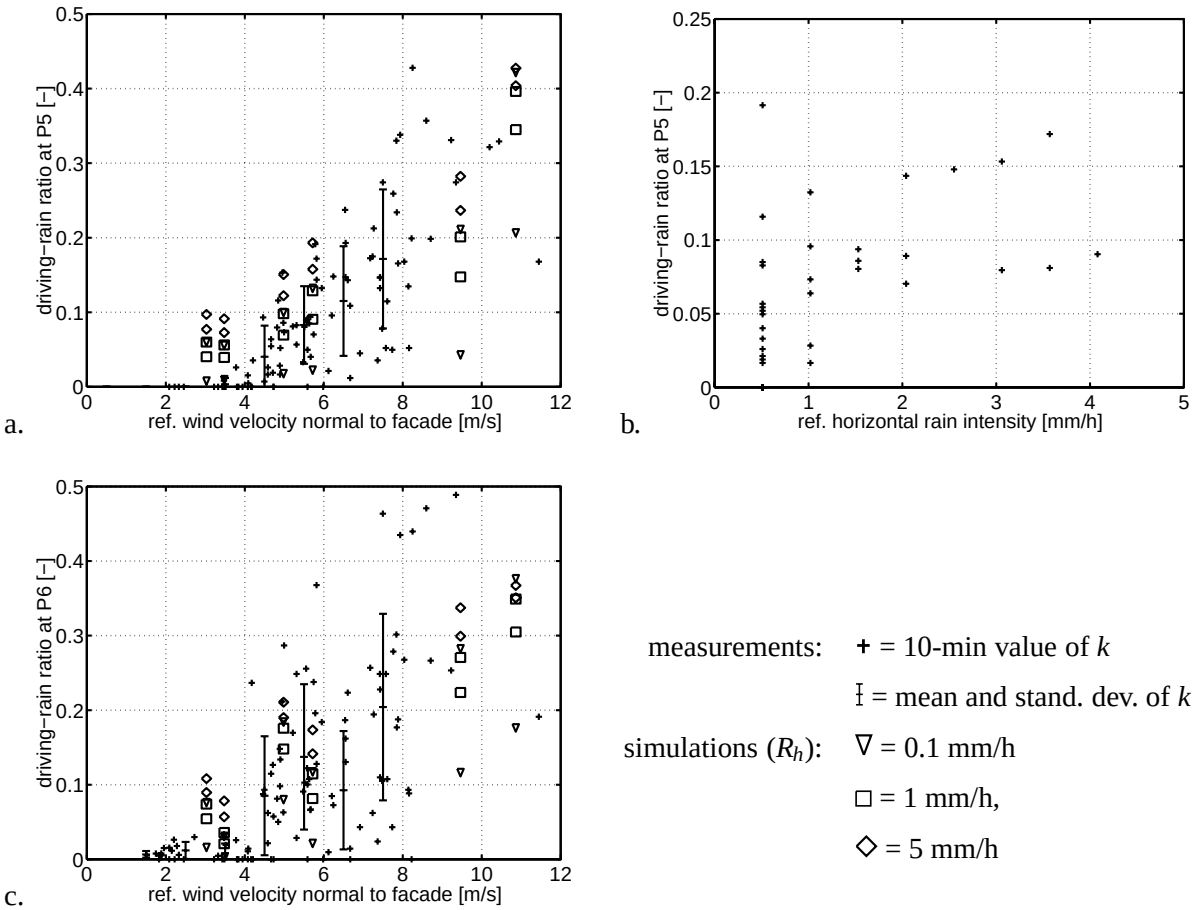

Figure 5: Measured and simulated driving rain ratios k at the facade position P5 and P6, as function of (a,c) the reference wind velocity compontent normal to the facade $U_{y,ref}$ and (b) the reference horizontal rain intensity R_h. Figures 5a and 5b refer to the central position P5; figure 5c refers to the edge position P6. Two different raindrop spectra have been applied for the calculation of k.

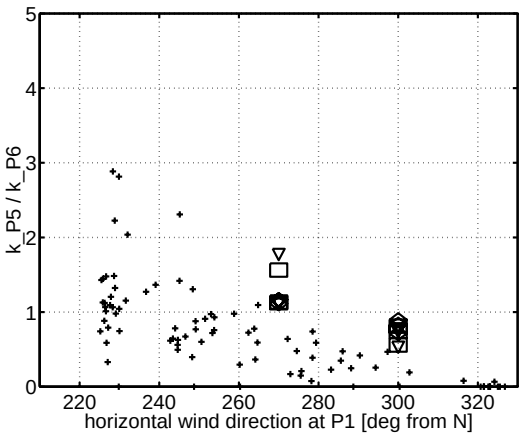

Figure 6: Measured and simulated quotients k_{P5}/k_{P6} at the facade position P5, as function of the reference wind direction Φ_{ref}. See the legend of figure 5.

ACKNOWLEDGEMENTS

This research is a joint project of the Faculty of Architecture, Planning and Building and of the Faculty of Technical Physics, at the TUE. The project is partly funded by the common TUE programme on 'Technology for Sustainable Development'. The fruitfull discussions with and the suggestions of dr. Marcel Bottema, dr.ir. Chris Geurts, prof.dr.ir. Klaas Kopinga, dr. Suresh Kumar M.Sc., prof.ir. Jacob Wisse and dr.ir. Martin de Wit are greatly acknowledged.

REFERENCES

BSI (1992). *BS 8104: Code of practice for assessing exposure of walls to wind-driven rain*. BSI.

Choi, E. (1993). Simulation of wind-driven-rain around a building. *Journal of Wind Engineering and Industrial Aerodynamics 46/47*, 721–729.

Fluent Inc. (1995). *Fluent user's guide; Version 4.3*. Fluent Inc.

Geurts, C. (1997). *Wind induced pressure fluctuations on building facades*. Ph. D. thesis, Eindhoven University of Technology.

Hangan, H. and D. Surry (1998). Wind-driven rain on buildings: A C-FD-E approach. In *Proceedings of the 4th UK Conference on Wind Engineering, Bristol (UK), 2–4 September 1998*, pp. 23–28. Wind Engineering Society.

Högberg, A., M. K. Kragh, and F. van Mook (1999). A comparison of driving rain measurements with different gauges. In *5th Symposium of Building Physics in the Nordic Countries, Göteborg (SE), 24–26 August*, pp. 361–368.

Karagiozis, A. and G. Hadjisophocleous (1996). Wind-driven rain on tall buildings. In *Proceedings of the 4th symposium on Building Physics in the Nordic Countries: Building Physics '96, Espoo (SF), 9–10 Sept.*, pp. 523–532. VTT Building Technology.

Marshall, J. and W. Palmer (1948). The distribution of raindrops with size. *Journal of Meteorology 5*, 165–166.

Murakami, S., A. Mochida, Y. Hayashi, and S. Sakamoto (1992). Numerical study on velocity-pressure field and wind forces for bluff bodies by k-ε, ASM and LES. *Journal of Wind Engineering and Industrial Aerodynamics 41-44*, 2841–2852.

Sankaran, R. and D. Paterson (1995). Computation of rain falling on a tall rectangular building. In *9th International Conference on Wind Engineering, New Delhi, India*, pp. 2127–2137. International Association for Wind Engineering.

Ulbrich, C. (1983). Natural variations in the analytical form of the raindrop size distribution. *Journal of Climate and Applied Meteorology 22*(10), 1764–1775.

van Mook, F. (1999). Full-scale measurements and numeric simulation of driving rain on a building fasade. In *Proceedings of the 10th International Conference on Wind Engineering. København (DK), 21-24 June*.

van Mook, F., M. de Wit, and J. Wisse (1997). Computer simulation of driving rain on building envelopes. In *Proceedings of the 2nd European and African Conference on Wind Engineering, 22-26 June 1997, Genova (IT)*, pp. 1059–1066.